

An Organic dye-sensitized tandem photoelectrochemical cell for light driven water splitting

Fusheng Li, Ke Fan, Bo Xu, Erik Gabrielsson, Quentin Daniel, Lin Li, and Licheng Sun

J. Am. Chem. Soc., **Just Accepted Manuscript** • DOI: 10.1021/jacs.5b04856 • Publication Date (Web): 01 Jul 2015

Downloaded from <http://pubs.acs.org> on July 9, 2015

Just Accepted

"Just Accepted" manuscripts have been peer-reviewed and accepted for publication. They are posted online prior to technical editing, formatting for publication and author proofing. The American Chemical Society provides "Just Accepted" as a free service to the research community to expedite the dissemination of scientific material as soon as possible after acceptance. "Just Accepted" manuscripts appear in full in PDF format accompanied by an HTML abstract. "Just Accepted" manuscripts have been fully peer reviewed, but should not be considered the official version of record. They are accessible to all readers and citable by the Digital Object Identifier (DOI®). "Just Accepted" is an optional service offered to authors. Therefore, the "Just Accepted" Web site may not include all articles that will be published in the journal. After a manuscript is technically edited and formatted, it will be removed from the "Just Accepted" Web site and published as an ASAP article. Note that technical editing may introduce minor changes to the manuscript text and/or graphics which could affect content, and all legal disclaimers and ethical guidelines that apply to the journal pertain. ACS cannot be held responsible for errors or consequences arising from the use of information contained in these "Just Accepted" manuscripts.



ACS Publications
High quality. High impact.

An organic dye-sensitized tandem photoelectrochemical cell for light driven total water splitting

Fusheng Li,^[a] Ke Fan,^[a] Bo Xu,^[a] Erik Gabrielsson,^[a] Quentin Daniel,^[a] Lin Li^[a] and Licheng Sun^{*[a, b]}

[a] Department of Chemistry, KTH Royal Institute of Technology, 110044 Stockholm, Sweden

[b] State Key Laboratory of Fine Chemicals, DUT–KTH Joint Education and Research Center on Molecular Devices
Dalian University of Technology (DUT), Dalian 116024, P. R. China

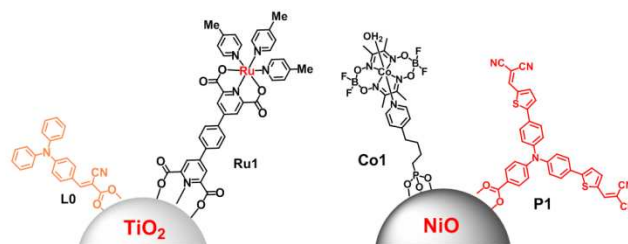
KEYWORDS: Photoelectrochemical (PEC) cell, Light driven water splitting, tandem cell, molecular catalyst, organic dyes.

ABSTRACT: Light driven water splitting was achieved by a tandem dye-sensitized photoelectrochemical cell with two photo-active electrodes. The photoanode is constituted by an organic dye **L0** as photosensitizer and a molecular complex **Ru1** as water oxidation catalyst on meso-porous TiO₂, while the photocathode is constructed with an organic dye **P1** as photo-absorber and a molecular complex **Co1** as hydrogen generation catalyst on nanostructured NiO. By combining the photocathode and the photoanode, this tandem DS-PEC cell can split water by visible light under neutral pH conditions without applying any bias.

Introduction

To satisfy our society for the global sustainable energy demands, utilizing solar energy to split water to produce hydrogen by photoelectrochemical (PEC) cell is one of the most promising strategies.^{1–3} Molecular catalysts have shown a great potential for the development of highly efficient water splitting devices due to their easy modification in structures, fine tuning in redox properties and high catalytic efficiencies.^{4–8} Recently, a series of molecular PEC cells for water splitting have been developed in our group.^{9–12} In these devices, Ru(bpy)₃ type photosensitizers were used together with molecular catalysts on TiO₂ as the photoanodes, and Pt as the cathode. In order to avoid the use of expensive metal Pt, a tandem molecular PEC cell was developed by our group,¹³ which showed a steady photocurrent density for water splitting under neutral pH conditions. This study indicates that Pt-free tandem molecular PEC cell can achieve total water splitting driven by visible light. However, the high cost of Ru-based photosensitizer is another limitation for the future large-scale application of this type of devices. Metal-free organic dyes have been widely used in dye-sensitized solar cells (DSSCs) due to their high efficiency, easy modification, tunable electron transfer process and low cost. They can be considered as the alternatives for Ru based photosensitizers in PEC devices.¹⁴ Recently, Finke et al. published an encouraging work in which perylene diimide served as an n-type semiconductor to drive CoO_x for water oxidation and a photocurrent of 150 $\mu\text{A cm}^{-2}$ was obtained,¹⁵ but a very high bias was required

(1V vs. Ag/AgCl) for this photoanode. Later, Mallouk et al. demonstrated a photoanode in which porphyrin dyes were used as photosensitizers to drive IrO_x for water oxidation, but the photocurrent density (less 50 $\mu\text{A cm}^{-2}$) and stability were not satisfactory.¹⁶ So far, no organic molecule showing better performance than Ru(bpy)₃ based dye for light-driving water splitting in PEC device was reported. Herein, we report a tandem PEC cell for total water splitting under neutral pH conditions, in which the photoanode is co-sensitized by a simple organic dye **L0** and Ru-based catalyst **Ru1** on meso-TiO₂, and the photocathode employs an organic dye **P1** and Co-based catalysts **Co1** co-sensitized on NiO, as shown in Scheme 1. This is the first case that organic dyes are employed as photosensitizers in both photoanode and photocathode of a tandem molecular PEC device for light driven total water splitting.



Scheme 1. The representation of the photoanode with organic dye **L0** and catalyst **Ru1** on TiO₂, and the photocathode with organic dye **P1** and catalyst **Co1** on NiO.

To make rational design of a tandem DS-PEC cell, several key issues should be considered. (i) the energy gap of the photoanode and the photocathode should match with each other. Here we use TiO_2 as photoanode material and NiO as photocathode material, which is similar to the design of tandem pn -DSSCs;¹⁷ (ii) the excited state of the n -type dye can inject an electron into the conduction band (CB) of TiO_2 from its lowest unoccupied molecular orbital (LUMO), while the excited state of the p -type dye can inject a hole into the valence band (VB) of NiO from its highest occupied molecular orbital (HOMO); (iii) for the photoanode the dye's oxidation potential E_{ox} should be more positive than the onset potential of water oxidation catalyst (WOC), while for the photocathode the dye's reduction potential E_{red} should be more negative than the onset potential of hydrogen generation catalyst (HGC); (iv) According to our previous study,¹¹ the distance between the dye and the surface of semiconductor should be shorter than the distance between the catalyst and the surface of semiconductor to facilitate the desired electron/hole injection and subsequent electron transfer.

Following the above considerations, the WOC **Ru1** [$\text{Ru}(\text{pdc})(\text{pic})_3$ with pyridine-2,6-dicarboxylic acid (pdc) as an anchoring group, $\text{pic} = 4$ -picoline] and the organic dye **L0** were immobilized on the surface of n -type TiO_2 film (8 μm thickness) for making the photoanode. Considering the organic dyes may form aggregates (dye island formation) and affect the device performance, the catalyst **Ru1** was adsorbed on TiO_2 first followed by the adsorption of **L0**. The loading amount of catalyst **Ru1** can be controlled by changing the concentration of **Ru1** and the loading time. Correspondingly, the HGC **Co1** [$\text{Co}(\text{dmgBF}_2)_2(\text{H}_2\text{O})$ with phosphonic acid as an anchoring group, $\text{dmgBF}_2 = \text{difluoroboryldimethylglyoximate}$] and the organic dye **P1** were immobilized on the surface of p -type NiO for the photocathode.

Experimental Section

Materials

All chemicals and solvents, if not stated, were purchased from Sigma Aldrich and used without further purification; water used in syntheses and measurements was deionized by Milli-Q technique. 4-hydroxy-2,6-pyridinedicarboxylic acid and 4-methylpyridine were purchased from TCI Development Co., Ltd. $\text{cis-Ru}(\text{DMSO})_4\text{Cl}_2$ and $\text{Co}(\text{dmgBF}_2)_2(\text{H}_2\text{O})_2$ were prepared according to published methods.^{18,19} Synthetic routes of **Ru1** and **Co1** can be found in supporting information.

General Electrochemical Methods

All electrochemical measurements were carried out using an Autolab potentiostat with a GPES electrochemical interface (Eco Chemie). An Ag/AgCl in 3 M KCl and a platinum foil were used as the reference electrode and the counter electrode, respectively. Using this reference electrode, all the potentials were converted to the NHE by using $[\text{Ru}(\text{bpy})_3]^{2+}/[\text{Ru}(\text{bpy})_3]^{3+}$ couple (Half-wave potential $E_{1/2} = 1.26$ V vs. NHE) as an internal reference. $E_{1/2}$ was determined by cyclic voltammetry as the average of the anodic and cathodic peak potentials ($E_{1/2} = (E_{\text{pa}} + E_{\text{pc}})/2$). To measure the electrochemical properties of catalysts on the metal oxide films, mix films were used due to the nature of TiO_2 and NiO . TiO_2 +ITO (ITO = indium tin

oxide, mass ratio 1:4) and NiO +ITO (mass ratio 1:4) were spin coated on FTO glasses, the films were calcinated at 450°C for 2h, then TiO_2 +ITO film and NiO +ITO film were dipped into **Ru1** solution, and **Co1** solution for 1h respectively, **Ru1**@ TiO_2 +ITO and **Co1**@ NiO +ITO electrodes were thus obtained.

Preparation of photoanode and photocathode

TiO_2 and NiO films were prepared according to our previous reports.^{10,20} The thicknesses of obtained bare TiO_2 film and NiO film are ca. 8 μm and 1 μm , respectively. The active areas of the photoelectrodes were 1 cm^2 . The bare TiO_2 film was dipped into 1 mM **Ru1** DCM (dichloromethane) solution for 15 min, after rinsed by MeOH the film was immersed in 1 mM **L0** DCM solution for 1h. The bare NiO film was dipped into 1 mM **P1** DCM solution for 5min. After rinsed by MeOH the film was immersed in 1 mM **Co1** for 1 h. The electrodes without loading photosensitizers or catalysts were prepared as well by using the same procedure as references.

Photoelectrochemical measurements

Photoelectrochemical measurements were carried out in phosphate buffer solution (pH 7, 50 mM Sigma Aldrich). In order to compare with our previous work,²¹ all tests were operated under light source of white LED light ($\lambda > 400$ nm, Color temperature 6000-6500 K, light intensity 100 mW cm^{-2}). To investigate the molecular photoanode and photocathode separately, conventional PEC cells were constructed by using photoanode or photocathode as working electrode, Pt net as counter electrode and Ag/AgCl electrode (3M KCl) as reference electrode. All the PEC cells were degassed by Ar or N_2 for 20 min before the photoelectrochemical measurements.

Determination of O_2 generation

The electrolyte in the PEC device was thoroughly degassed by N_2 . The volumes of the solution and the headspace in the working compartment were measured. To evaluate oxygen generation, 0.5 mL gas phase of the headspace was transferred into a gas chromatography (GC) using a Hamilton SampleLock syringe. GC-2014, Shimadzu Molecular sieve 5A, TCD detector, nitrogen as the carry gas was used to measure the H_2 evolution, and with helium as a carrier gas was used to measure the O_2 evolution.

IPCE measurements

Incident photon to current conversion efficiency (IPCE) spectra was obtained by illumination of the photoelectrodes with light of a specific wavelength (from 370 nm to 650 nm) and measuring the resulting short-circuit current. The currents were recorded using a computer-controlled setup consisting of potentiostat (EG&GPAR 273). The illumination was supplied by a Xenon light source (Spectral Products ASB-XE-175) and calibrated using a certified reference solar cell (Fraunhofer ISE). The specific wavelength was controlled by a monochromator (Spectral Products CM110).

Results and discussion

From cyclic voltammetry curves of **Ru1**@ TiO_2 +ITO and **Co1**@ NiO +ITO electrodes (Figure S4 and S5), the onset potentials of WOC and HGC can be determined, the E_{onset} of **Ru1**

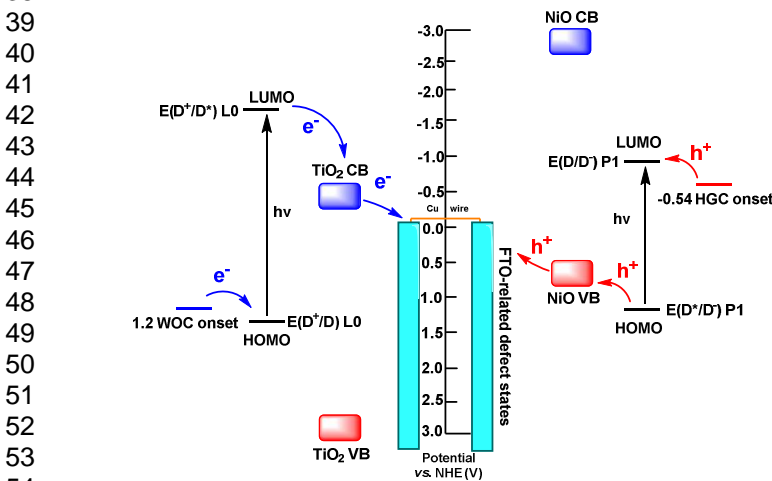
for water oxidation is around 1.2 V vs. NHE, and the E_{onset} of **Co1** for hydrogen generation is around -0.54V vs. NHE. The organic dyes **L0** and **P1** have been reported in DSSCs.²²⁻²⁴ Corresponding optical and electrochemical properties of the dyes and the catalysts are shown in Table 1.

According to the electrochemical properties of the dyes, the catalysts and the semiconductors,^{17,25} a schematic energy diagram was illustrated in Scheme 2. After illumination of the photoanode, the excited state of dye **L0** can inject an electron into the CB of TiO₂ and the photo-generated **L0**⁺ can oxidize the catalyst **Ru1**, leading to water oxidation after repeating multi-electron transfer processes. Meanwhile, at the photocathode, the excited state **P1** can inject hole into the VB of NiO and the formed **P1**⁻ which can reduce the catalyst **Co1** for eventual hydrogen generation.

Table 1. Optical and Electrochemical Properties of the Dyes and Catalysts

Dyes and Catalysts	$\lambda_{abs}(\epsilon/M^{-1}cm^{-1})$ / nm	λ_{em} / nm	$E_{ox}(HOMO)$ / V vs. NHE	E_{0-0} / eV	LUMO / V vs. NHE
P1	348(34720);481(57900)	618	1.32	2.25	- 0.93
L0	373 387(36000)	509	1.37	2.90	-1.53
Ru1	Ru1 onset potential for water oxidation on TiO ₂ is around 1.20 V				
Co1	Co1 onset potential for hydrogen generation on NiO is around -0.54 V				

First, linear scan voltammetry (LSV) of **L0+Ru1@TiO₂** under illumination (Figure 1) showed that the photocurrent rapidly increased with the applied potential from -0.25 V to -0.15 V (vs. NHE), and reached a plateau at $E > -0.1$ V with a photocurrent density of 0.42 mA cm⁻². This value is significantly higher in comparison to the current densities under dark condition, indicating that the working electrode is indeed photoactive. From LSV, the relationship between the applied bias potential and photocurrent can be found, here 0 V vs. Ag/AgCl as the applied bias was selected to measure the photocurrent of **L0+Ru1@TiO₂** electrode.



Scheme 2. Schematic energy diagram for **L0**, **P1**, **Ru1**, **Co1**, FTO, TiO₂ and NiO (all data shown at pH 7).

Transient current responses to on-off cycles and full time photocurrent under illumination were then studied and results are shown in Figure 2. For **L0+Ru1@TiO₂** pho-

toanode, it produced a remarkable average photocurrent of ca. 300 $\mu A\ cm^{-2}$. For the **L0@TiO₂** photoanode without the catalyst **Ru1**, it only produced ca. 30 $\mu A\ cm^{-2}$ photocurrent density under the same conditions, while for **Ru1@TiO₂** electrode only an indistinct photocurrent can be achieved (Figure S8). **Ru1** have a strong absorption of visible light (Figure S6), but it will be hard for **Ru1** to inject 4 electrons into TiO₂ and generate Ru^V species for water oxidation. The significant increase of photocurrent confirms the highly catalytic activity of **Ru1** for water oxidation, and the electron transfer from the catalyst to the oxidized dye should occur as anticipated. In comparison to our previous study on similar PEC device using the catalyst **Ru1** and Ru(bpy)₃ based photosensitizer as photoanode (giving

photocurrent density of ca. 100 $\mu A\ cm^{-2}$),¹³ the higher photocurrent density obtained from the photoanode **L0+Ru1@TiO₂** indicates that this simple organic dye **L0** based device exhibits much better device performance than the expensive Ru(bpy)₃ photosensitizer based device. Additionally, compared with photoanodes developed by Finke and Mallouk,^{15,16} our photoanode **L0+Ru1@TiO₂** shows advances of low applied bias potential and high current density.

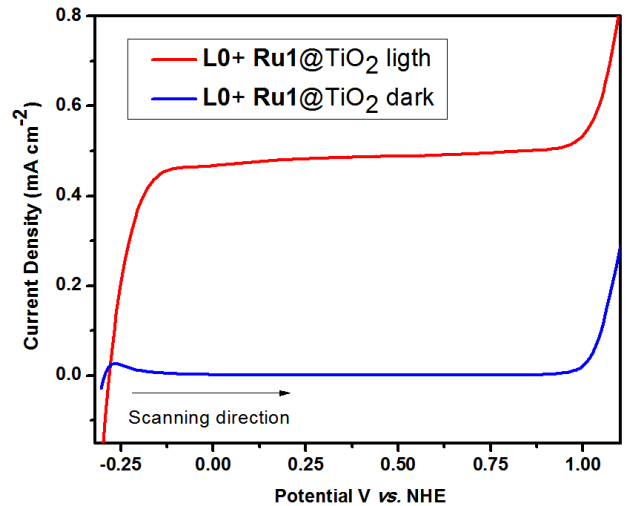


Figure 1. LSV measurements of the WEs under light illumination (light intensity 100 mW cm⁻²), scan rate = 50 mV s⁻¹, in a three-electrode PEC cell with Pt as counter electrode, Ag/AgCl as reference electrode, operated in a 50 mM pH 7.0 phosphate buffer solution.

In a long term illumination experiment the photoanode **L0+Ru1@TiO₂** showed a relatively slow decay of photocur-

rent (Figure 2 and S10). It's well known that the stability of molecular PEC cells is usually poor.¹⁰⁻¹² One of the main reasons is that molecular catalysts or dyes could detach from the metal oxide surface in the presence of electrolyte solution, which leads to a drastically decay of the photocurrent. In our case, pyridine-2,6-dicarboxylic acid was used as the anchoring group of the catalyst **Ru1** which is exceptionally strong in comparison to the commonly used carboxylic acid and phosphonic acid,^{13,26} no obvious desorption of the catalyst **Ru1** from the surface of TiO_2 can be observed with pH ranging from pH 1 to pH 14. The organic dye **L0** is insoluble in water, which also can hinder the desorption from the surface of TiO_2 . Due to these reasons, our photoanode **L0+Ru1@TiO₂** shows a much better stability.

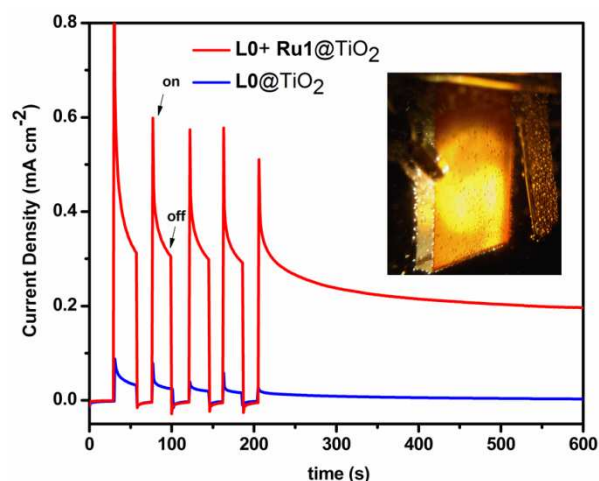


Figure 2. The transient current responses to on-off cycles and full time photocurrent of illumination (light intensity 100 mW cm^{-2}) on photoanodes under an applied bias potential of 0 V vs. Ag/AgCl in a **three-electrode** PEC cell with Pt as counter electrode, operated in a 50 mM pH 7.0 phosphate buffer solution.

During 60 min illumination, bubbles are formed on the photoanode surface (inset of Figure 2 and Figure S9), the photo-generated oxygen gas was confirmed by gas chromatography (GC), 0.46 C charges passed through the electrode (Figure S10), $0.87 \mu\text{mol O}_2$ was detected by GC, and the faraday efficiency was calculated to be 73%. More interestingly, with long time illumination on photoanode in two-electrode system (**L0+Ru1@TiO₂** 0.4 cm^2 as working electrode and Pt net as counter electrode) without applying any bias, the PEC cell can still generate oxygen which was detected by Clark-electrode (Figure S11). For the photoanode with **L0** alone (**L0@TiO₂**), only 15 nmol mL^{-1} oxygen was generated after 30 min illumination. For the photoanode with **Ru1** alone, almost no oxygen can be detected. In contrast, for **L0+Ru1@TiO₂** electrode 140 nmol mL^{-1} oxygen was obtained after 30 min illumination. These results clearly prove that the light-driven water oxidation is successfully achieved by assembly with catalyst **Ru1** and organic photosensitizer **L0** on TiO_2 .

For preparing the photocathode, a cobalt complex **Co1** with an anchoring group was employed as the hydrogen generation catalyst and organic dye **P1** was used as photosensitizer, and they were immobilized on NiO film. Since the NiO film used here was very thin ($1 \mu\text{m}$ in thickness), **P1** was adsorbed before **Co1** to make sure more dyes can be loaded on the elec-

trode. LSV experiments on the assembled **P1+Co1@NiO** photocathode show that, under illumination, the photocurrent rapidly increased with the applied potential from 0.4 V to -0.1 V (vs. NHE), and reached a plateau at $E < -0.1 \text{ V}$ with a photocurrent density of ca. $-45 \mu\text{A cm}^{-2}$ (Figure 3).

The transient current responses to on-off cycles show that at -0.2 V vs. Ag/AgCl applied potential the **P1+Co1@NiO** photocathode can produce an average photocurrent of ca. $-35 \mu\text{A cm}^{-2}$, while the reference photocathode **P1@NiO** without the catalyst **Co1** produced only $-4 \mu\text{A cm}^{-2}$ current density under the same condition (Figure 4), while for **Co1@NiO** electrode only an indistinct photocurrent can be observed (Figure S12). Compared to our previous work where **P1** and $[\text{Co}(\text{dmgBF}_2)_2(\text{H}_2\text{O})_2]$ were encapsulated on NiO film,²¹ the photostability of the present device was significantly improved. This means the phosphonic acid anchoring group in the catalyst **Co1** benefits for the photostability of this PEC device. After 90 min illumination, a photocurrent density of $-20 \mu\text{A cm}^{-2}$ maintains (Figure S13). The photo-generated hydrogen gas was confirmed by GC, 0.082 C charges passed the electrode. $0.29 \mu\text{mol H}_2$ was detected, giving a Faraday efficiency of 68%.

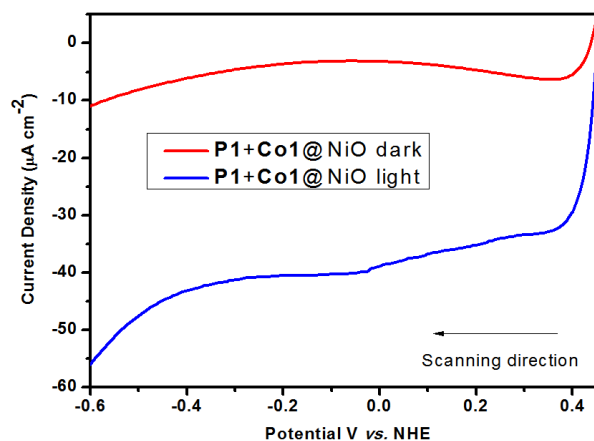


Figure 3. LSV measurements of the WEs under light illumination (light intensity 100 mW cm^{-2} , scan rate = 50 mV s^{-1}), in a **three-electrode** PEC cell with Pt as counter electrode, Ag/AgCl as reference electrode, operated in a 50 mM pH 7.0 phosphate buffer solution.

With both functional photoanode and photocathode in hands, we have prepared a tandem PEC cell with **two-electrode** configuration. The working electrode (WE) is the **P1+Co1@NiO** photocathode, and the counter electrode (CE) is the **L0+Ru1@TiO₂** photoanode. The direction of the light illumination on photo-electrode was essential to the performance of the PEC cell. Three configurations were performed by different illumination ways, as shown in Figure 5. In **configuration 1**, both electrodes are simultaneously illuminated and the best performance was obtained.

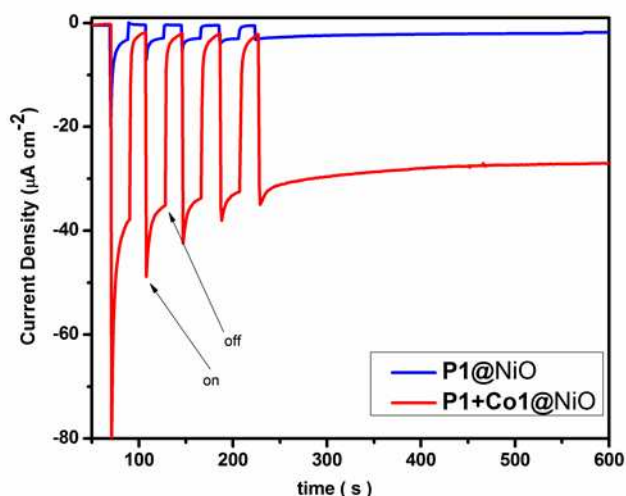
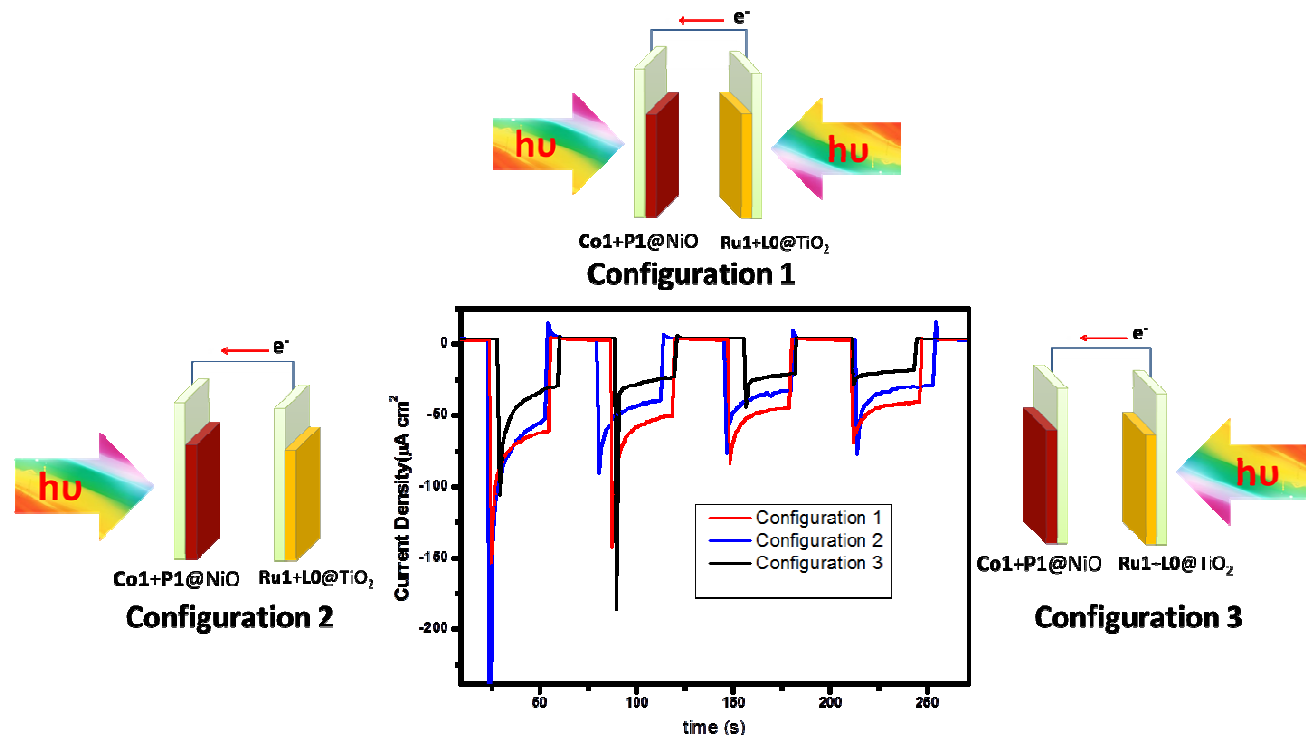


Figure 4. The transient current responses to on-off cycles and full time photocurrent of illumination (light intensity 100 mW cm⁻²) on photocathodes under an applied potential of -0.2 V vs. Ag/AgCl in a **three-electrode** PEC cell with Pt as counter electrode, operated in a 50 mM pH 7.0 phosphate buffer solution.

cell is thicker than the NiO film (1 μm), the light can go through NiO film first and more remaining light can reach the TiO₂ film. Considering **configuration 1** is the best illumination way for PEC cell in our case, thus **configuration 1** was therefore selected to test the performances of this tandem PEC cell.

From LSV experiments on **P1+Co1@NiO/L0+Ru1@TiO₂** PEC cell, it was found that the photocurrent rapidly increased with the changing of applied potential from 0.8 V to 0.6 V (vs. NHE), and reached a plateau at $E < 0.6$ V with a photocurrent density of ca. -70 μA cm⁻² (as shown in Figure 6). It is clearly shown this tandem PEC cell can work without any applied bias. Transient current responses to on-off cycles and full time photocurrent under illumination without bias were studied (Figure 7). First, the photocurrent density of **P1+Co1@NiO/Pt** in two-electrode setup was much lower (5 μA cm⁻², Figure 7 blue) than the three-electrode setup one (35 μA cm⁻², Figure 4 red). This behavior can be explained as follows, in two-electrode setup, the valence band of NiO is located around 0.5 V vs. NHE, which is not high enough to drive water oxidation, that's why the **P1+Co1@NiO/Pt** PEC cell almost does not work. While, in three-electrode setup, the Pt counter electrode can get extra potential from electrochemical workstation for water oxidation. Second, for the tandem cell (**P1+Co1@NiO/L0+Ru1@TiO₂**), the photocurrent density



Figure

5. The transient current responses to on-off cycles of a tandem PEC device in **two-electrode** setup with different directions of the light illumination (without any applied potential).

When the light is illuminated from the **P1+Co1@NiO** side (**configuration 2**), the tandem PEC cell exhibits better performance than that of **configuration 3** where the light is illuminated from the **L0+Ru1@TiO₂** side. The reason is probably due to the overlap of the absorption regions of **L0** and **P1** (Figure S6 and S7). As the TiO₂ film (8 μm) used in this PEC

shows a significant enhancement (ca 70 μA cm⁻²) compared to **P1+Co1@NiO/Pt**. This enhancement was due to the replacement of Pt by **L0+Ru1@TiO₂** photoanode, in this case, the photo-generated electrons and holes can flow in this PEC cell as shown in Scheme 2. The difference between **P1+Co1@NiO/Pt** and **P1+Co1@NiO/L0+Ru1@TiO₂** PEC

cells indicates that a good photoanode can not only provide protons for the hydrogen generation half-reaction, but also can assist the charge flow between two electrodes, which means good design of photoanode is quite necessary and important for tandem PEC cells.

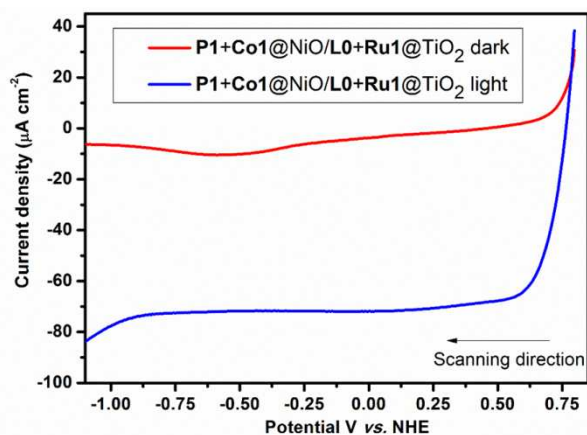


Figure 6. LSV measurements of the WEs under light illumination (light intensity 100 mW cm^{-2} , scan rate = 50 mV s^{-1} , in a two-electrode PEC cell as configuration 1.

From full time photocurrent measurement on this tandem PEC cell, we found a relatively slow photocurrent decay (ca 60% photocurrent remained after 10 min illumination). Photo-generated hydrogen was collected and measured by GC from the tandem PEC cell (**P1+Co1@NiO/L0+Ru1@TiO₂**) with two-electrode setup and without external bias for 100 min illumination (using a two-compartment cell divided by a glass frit as shown in Figure S1). $0.33 \mu\text{mol H}_2$ was produced with 0.117 C (Figure S2) of charges passed through the electrodes, which corresponds to 55% Faraday efficiency. These observed Faraday efficiencies for **P1+Co1@NiO** (in three-electrode setup) and **P1+Co1@NiO/L0+Ru1@TiO₂** (in two-electrode setup) are similar to those reported in literature.²⁷ However, we believe that the Faraday efficiency was underestimated in our case, although two-compartment cell divided by glass frit was used, some of the molecular O_2 and H_2 generated in each compartment can be dissolved in the solution, and then diffuse to the other compartment for respective reduction and oxidation, resulting in the low observed Faraday efficiency.

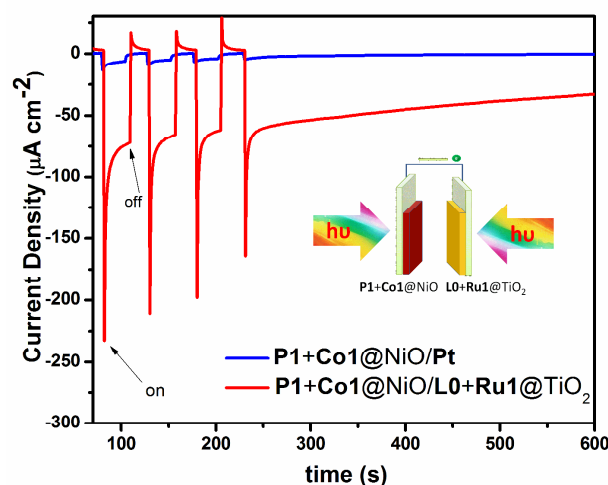


Figure 7. The transient current responses to on-off cycles and full time photocurrent of illumination on photoelectrodes in two-electrode setups without any bias, **P1+Co1@NiO** as WE, Pt or **L0+Ru1@TiO₂** as CE. Operated in a 50 mM pH 7.0 phosphate buffer solution (light intensity 100 mW cm^{-2}).

With the Faraday efficiency, the performance of the tandem PEC cell can be assessed by the corresponding solar-to-hydrogen conversion efficiency η_{STH} with equation (1),²⁸⁻³⁰ where J_{op} is the effective operating current density measured during device operation ($70 \mu\text{A cm}^{-2}$), V is the water splitting potential required (1.23 V), V_{bias} is the bias voltage that can be added in series with the two electrodes (0 V), P_{light} is the incident light power (100 mW cm^{-2}), η_{F} is Faraday efficiency (55%). According to equation (1), η_{STH} of this tandem device is calculated to be 0.05%.

$$\eta_{\text{STH}} = \frac{(J_{\text{op}} [\text{mA cm}^{-2}] \times (V_{\text{water splitting}} - V_{\text{bias}}) \times \eta_{\text{F}})}{P_{\text{light}} [\text{mW cm}^{-2}]} \quad (1)$$

A monochromatic incident photon-to-electron conversion efficiency (IPCE) measurement was performed, due to the limitation of experimental conditions, the IPCE of **Configuration 1** is very challenging to measure. As shown in Figure 5, **Configuration 2** displays a comparable performance to **Configuration 1**, so the IPCE of this tandem PEC cell was performed by using **Configuration 2**. As shown in Figure 8, the tandem PEC cell (**P1+Co1@NiO/L0+Ru1@TiO₂**) shows an IPCE of 25.2% at 380 nm (max_{abs} of **L0**), 3.9% at 480 nm (max_{abs} of **P1**). This IPCE indicates both **L0** and **P1** contribute for the photon-to-electron conversion in this tandem PEC cell, this is an advantage of using the concept of dye-sensitized photoelectrodes with different dyes to achieve a broader absorption of visible light.

It's known that NiO has a poor hole mobility as p-type semiconductor,³¹ and short hole diffusion length, leading to fast charge recombination.³² At the same time, it's difficult to prepare thicker NiO films to load more dyes and catalysts.^{31,33} Our IPCE data also indicates our photoanode can convert more light into electrons than that of photocathode. And the photocurrent generated by **P1+Co1@NiO** is much lower than that of **L0+Ru1@TiO₂** (Figure 2 and 4), these indicate that the NiO based photocathode is the bottleneck of this tandem cell. However it is believed that with the development of new p-

type semiconductors and new routes to prepare thicker films, better PEC devices can be prepared with this type of tandem DS-PEC cell design.

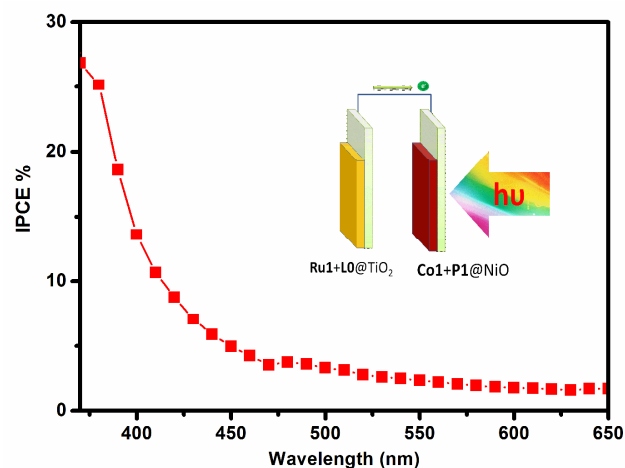


Figure 8. The IPEC spectra of **Configuration 2** in 50 mM pH 7 phosphate buffer, in **two-electrode** setup without applying any bias voltage (data points are from average of three independent experiments).

Conclusion

In summary, an n-type organic dye **L0** co-absorbed with a molecular water oxidation catalyst **Ru1** on TiO_2 was used for preparation of a photoanode, and visible light driven water oxidation by using this photoanode was successfully achieved. The photoanode **L0+Ru1@TiO₂** can produce a remarkable average photocurrent of $300 \mu\text{A cm}^{-2}$ under pH 7 neutral conditions. A hydrogen generation catalyst **Co1** co-sensitized with an organic dye **P1** on NiO was used for a photocathode. Both photocurrent and photo-stability of this photocathode were improved compared to previous reported systems. A tandem DS-PEC cell was designed and prepared by connecting the above mentioned photoanode and photocathode. For the first time, a metal free organic dyes sensitized tandem PEC cell can split water by visible light with IPCE of 25% at 380 nm under neutral pH conditions without bias. These results provide a new guidance for the design of molecular PEC cells, leading to a great promise to construct low-cost Pt-free devices for artificial photosynthesis in the future.

ASSOCIATED CONTENT

Supporting Information

Synthesis of molecules, NMR, MS, IR, UV-Vis and electrochemical measurement details are included in the supporting information. This material is available free of charge via the internet at <http://pubs.acs.org>.

AUTHOR INFORMATION

Corresponding Author

Prof. Licheng Sun, KTH
E-mail: lichengs@kth.se

Notes

The authors declare no competing financial interests.

ACKNOWLEDGMENT

We acknowledge the financial support of this work by the Swedish Energy Agency, the Knut and Alice Wallenberg Foundation, the Swedish Research Council, the National Natural Science Foundation of China (21120102036, 91233201), the National Basic Research Program of China (973 program, 2014CB239402) and China Scholarship Council.

REFERENCES

- (1) Gratzel, M. *Nature* **2001**, *414*, 338.
- (2) Walter, M. G.; Warren, E. L.; McKone, J. R.; Boettcher, S. W.; Mi, Q.; Santori, E. A.; Lewis, N. S. *Chem. Rev.* **2010**, *110*, 6446.
- (3) Tachibana, Y.; Vayssieres, L.; Durrant, J. R. *Nat. Photon.* **2012**, *6*, 511.
- (4) Yagi, M.; Kaneko, M. *Chem. Rev.* **2000**, *101*, 21.
- (5) Francàs, L.; Bofill, R.; García-Antón, J.; Escriche, L.; Sala, X.; Llobet, A. In *Molecular Water Oxidation Catalysis*; John Wiley & Sons, Ltd: 2014, p 29.
- (6) Duan, L.; Tong, L.; Xu, Y.; Sun, L. *Energy Environ. Sci.* **2011**, *4*, 3296.
- (7) Imahori, H. *ChemSusChem* **2015**, *8*, 426.
- (8) Yu, Z.; Li, F.; Sun, L. *Energy Environ. Sci.* **2015**, *8*, 760.
- (9) Li, L.; Duan, L. L.; Xu, Y. H.; Gorlov, M.; Hagfeldt, A.; Sun, L. C. *Chem. Commun.* **2010**, *46*, 7307.
- (10) Gao, Y.; Ding, X.; Liu, J. H.; Wang, L.; Lu, Z. K.; Li, L.; Sun, L. C. *J. Am. Chem. Soc.* **2013**, *135*, 4219.
- (11) Gao, Y.; Zhang, L.; Ding, X.; Sun, L. *Phys. Chem. Chem. Phys.* **2014**, *16*, 12008.
- (12) Zhang, L.; Gao, Y.; Ding, X.; Yu, Z.; Sun, L. *ChemSusChem* **2014**, *7*, 2801.
- (13) Fan, K.; Li, F.; Wang, L.; Daniel, Q.; Gabrielsson, E.; Sun, L. *Phys. Chem. Chem. Phys.* **2014**, *16*, 25234.
- (14) O'Regan, B.; Gratzel, M. *Nature* **1991**, *353*, 737.
- (15) Kirner, J. T.; Stracke, J. J.; Gregg, B. A.; Finke, R. G. *ACS Appl. Mater. Interfaces* **2014**, *6*, 13367.
- (16) Swierk, J. R.; Méndez-Hernández, D. D.; McCool, N. S.; Liddell, P.; Terazono, Y.; Pahk, I.; Tomlin, J. J.; Oster, N. V.; Moore, T. A.; Moore, A. L.; Gust, D.; Mallouk, T. E. *Proc. Natl. Acad. Sci. U. S. A.* **2015**, *112*, 1681.
- (17) Nattestad, A.; Mozer, A. J.; Fischer, M. K. R.; Cheng, Y. B.; Mishra, A.; Bauerle, P.; Bach, U. *Nat. Mater.* **2010**, *9*, 31.
- (18) Alessio, E.; Mestroni, G.; Nardin, G.; Attia, W. M.; Calligaris, M.; Sava, G.; Zorzet, S. *Inorg. Chem.* **1988**, *27*, 4099.
- (19) Bakac, A.; Espenson, J. H. *J. Am. Chem. Soc.* **1984**, *106*, 5197.
- (20) Li, L.; Gibson, E. A.; Qin, P.; Boschloo, G.; Gorlov, M.; Hagfeldt, A.; Sun, L. C. *Adv. Mater.* **2010**, *22*, 1759.
- (21) Li, L.; Duan, L.; Wen, F.; Li, C.; Wang, M.; Hagfeldt, A.; Sun, L. *Chem. Commun.* **2012**, *48*, 988.
- (22) Hagberg, D. P.; Marinado, T.; Karlsson, K. M.; Nonomura, K.; Qin, P.; Boschloo, G.; Brinck, T.; Hagfeldt, A.; Sun, L. *J. Org. Chem.* **2007**, *72*, 9550.
- (23) Qin, P.; Zhu, H.; Edvinsson, T.; Boschloo, G.; Hagfeldt, A.; Sun, L. *J. Am. Chem. Soc.* **2008**, *130*, 8570.
- (24) Kitamura, T.; Ikeda, M.; Shigaki, K.; Inoue, T.; Anderson, N. A.; Ai, X.; Lian, T.; Yanagida, S. *Chem. Mater.* **2004**, *16*, 1806.
- (25) Liang, Y.; Tsubota, T.; Mooij, L. P. A.; van de Krol, R. *J. Phys. Chem. C* **2011**, *115*, 17594.
- (26) Gabrielsson, E.; Tian, H.; Eriksson, S. K.; Gao, J.; Chen, H.; Li, F.; Oscarsson, J.; Sun, J.; Rensmo, H.; Kloo, L.; Hagfeldt, A.; Sun, L. *Chem. Commun.* **2015**, *51*, 3858.
- (27) Ji, Z.; He, M.; Huang, Z.; Ozkan, U.; Wu, Y. *J. Am. Chem. Soc.* **2013**, *135*, 11696.
- (28) Van de Krol, R.; Schoonman, J. In *Sustainable Energy Technologies*; Hanjalic, K.; Van de Krol, R.; Lekić, A., Eds.; Springer Netherlands: 2008, p 121.
- (29) van de Krol, R.; Liang, Y.; Schoonman, J. *J. Mater. Chem.* **2008**, *18*, 2311.
- (30) Hisatomi, T.; Kubota, J.; Domen, K. *Chem. Soc. Rev.* **2014**, *43*, 7520.
- (31) Morandeira, A.; Fortage, J.; Edvinsson, T.; Le Pleux, L.; Blart, E.; Boschloo, G.; Hagfeldt, A.; Hammarström, L.; Odobel, F. *J. Phys. Chem. C* **2008**, *112*, 1721.

- (32) Mori, S.; Fukuda, S.; Sumikura, S.; Takeda, Y.; Tamaki, Y.; Suzuki, E.; Abe, T. *J. Phys. Chem. C* **2008**, *112*, 16134.
(33) Lepleux, L.; Chavillon, B.; Pellegrin, Y.; Blart, E.; Cario, L.; Jobic, S.; Odobel, F. *Inorg. Chem.* **2009**, *48*, 8245.

Contents artwork

